HAL open science

In situ Analytical Quality Control of chemotherapeutic solutions in infusion bags by Raman spectroscopy

Alaa Makki, Suha Elderderi, Victor Massot, Renaud Respaud, Hugh.J. Byrne, Clovis Tauber, Dominique Bertrand, Elhadi Mohammed, Igor Chourpa, Franck Bonnier

To cite this version:

Alaa Makki, Suha Elderderi, Victor Massot, Renaud Respaud, Hugh.J. Byrne, et al.. In situ Analytical Quality Control of chemotherapeutic solutions in infusion bags by Raman spectroscopy. Talanta, 2021, 228, pp.122137. 10.1016/j.talanta.2021.122137 . hal-03376371

HAL Id: hal-03376371

https://univ-tours.hal.science/hal-03376371v1

Submitted on 9 Mar 2023

HAL is a multi-disciplinary open access archive for the deposit and dissemination of scientific research documents, whether they are published or not. The documents may come from teaching and research institutions in France or abroad, or from public or private research centers.

L'archive ouverte pluridisciplinaire **HAL**, est destinée au dépôt et à la diffusion de documents scientifiques de niveau recherche, publiés ou non, émanant des établissements d'enseignement et de recherche français ou étrangers, des laboratoires publics ou privés.

Distributed under a Creative Commons Attribution - NonCommercial 4.0 International License

Version of Record: https://www.sciencedirect.com/science/article/pii/S0039914021000588
Manuscript_98accbbd5235a046fa40d486f4de7598

In situ Analytical Quality Control of chemotherapeutic solutions in infusion bags by Raman spectroscopy

Alaa A. Makki[a, b], Suha Elderderi[a, b], Victor Massot[c], Renaud Respaud[d], Hugh. J. Byrne[e], Clovis Tauber[f], Dominique Bertrand[g], Elhadi Mohammed[h], Igor Chourpa[a], Franck Bonnier [a,*]

[a] Université de Tours, EA 6295 Nanomédicaments et Nanosondes, 31 avenue Monge, 37200 Tours, France

[b] University of Gezira, Faculty of Pharmacy, Department of Pharmaceutical Chemistry, P.O. Box 20, 21111 Wad Madani, Sudan

[c] CHU de Tours, Unité de Biopharmacie Clinique Oncologique, Pharmacie, France.

[d] Université de Tours, UMR 1100, CHRU de Tours, Service de Pharmacie, F-37032 Tours, France

[e] FOCAS Research Institute, TU Dublin, City Campus, Kevin Street, Dublin 8, Ireland

[f] Université de Tours, INSERM UMR 1253 iBrain, 37000 Tours, France.

[g] Data_Frame, 25 rue Stendhal, 44300 Nantes, France

[h] University of Gezira, Faculty of Pharmacy, Medicinal and Aromatic Plants Research Center (MAPRC), P.O. Box 20, 21111 Wad Madani, Sudan

Corresponding author:

Dr. Franck Bonnier

University of Tours, faculty of pharmacy

EA 6295 NMNS

31 Avenue Monge

37200 Tours, France

Key words:

Confocal Raman micro-spectroscopy, Chemotherapeutics, non-invasive analysis, analytical quality control

© 2021 published by Elsevier. This manuscript is made available under the CC BY NC user license
https://creativecommons.org/licenses/by-nc/4.0/

Abstract

Analytical Quality Control (AQC) in centralised preparation units of oncology centres is a common procedure relying on the identification and quantification of the prepared chemotherapeutic solutions for safe intravenous administration to patients. Although the use of Raman spectroscopy for AQC has gained much interest, in most applications it remains coupled to a flow injection analyser (FIA) requiring withdrawal of the solution for analysis. In addition to current needs for more rapid and cost-effective analysis, the risk of exposure of clinical staff to the toxic molecules during daily handling is a serious concern to address. Raman spectroscopic analysis, for instance by Confocal Raman Microscopy (CRM), could enable direct analysis (non-invasive) for AQC directly in infusion bags. In this study, 3 anticancer drugs, methotrexate (MTX), 5-fluorouracil (5-FU) and gemcitabine (GEM) have been selected to highlight the potential of CRM for withdrawal free analysis. Solutions corresponding to the clinical range of each drug were prepared in 5% glucose and data was collected from infusion bags placed under the Raman microscope. Firstly, 100% discrimination has been obtained by Partial Least Squares Discriminant Analysis (PLS-DA) confirming that the identification of drugs can be performed. Secondly, using Partial Least Squares Regression (PLSR), quantitative analysis was performed with mean % error of predicted concentrations of respectively 3.31%, 5.54% and 8.60% for MTX, 5-FU and GEM. These results are in accordance with the 15% acceptance criteria used for the current clinical standard technique, FIA, and the Limits of Detection for all drugs were determined to be substantially lower than the administered range, thus highlighting the potential of confocal Raman spectroscopy for direct analysis of chemotherapeutic solutions.

1. Introduction

Increasingly, preparation of chemotherapeutic drugs is centralised in dedicated units in hospitals, to reduce cost and waste generated during reconstitution of individualised doses, but also to increase the security in the process from the receipt of commercial stock products (highly concentrated liquid or powder) to their release to patient bedsides [1]. Meanwhile, in recent years, concepts of personalised medicine have considerably increased the complexity and precision of prescriptions, for example, for complex anticancer treatment protocols.

The control of chemotherapy is compulsory with at least double visual inspection (non-analytical control) but there is no consensus on the methods to be applied [2]. Analytical Quality Control (AQC) is one of the potential methodological frameworks and is widely used in large oncology centers for chemotherapeutic preparations because it enables both the qualitative (identification) and quantitative analysis of the solutions assayed [3].

Among the AQC techniques used, chromatographic methods such as high-performance liquid chromatography (HPLC) remain the gold standard for quality control of chemotherapeutic preparations for qualitative and quantitative analysis [3–6]. QC can be a very time consuming and costly control method (consumables, solvents), although it is expected that the analysis is reliable and rapid, allowing prompt release of the treatment without impacting patient planning. Therefore, alternative approaches using vibrational spectroscopic techniques have been developed in recent years to propose cost effective and rapid alternatives to identify and quantify the anticancer drug within their solubilisation matrices [4].

Vibrational spectroscopic techniques, namely infrared (IR) and Raman spectroscopy, are structure specific techniques delivering molecular fingerprints. The techniques are label free, non-invasive and non-destructive, require no separation of chemical species prior to analysis, no sample preparation and as a result they are less demanding, consumables wise (solvent, column, etc.). IR and Raman spectroscopy have several applications in medical, biomedical and biopharmaceutical sciences as well as in forensic medicine [7–16]. In the context of AQC of chemotherapeutic solutions, it has been demonstrated that coupling vibrational techniques with multivariate analysis enables qualitative (identification of drug) and quantitative analysis [17,18].

Originally, the first dedicated instruments commercialised for qualitative and quantitative analysis of chemotherapeutic preparations were performed using a system coupling Fourier transform infrared spectroscopy (FTIR) to UV/vis spectrometry (Multispec® analyser, Microdom, Taverny, France) [19–22]. Despite the well-known limitation due to water

absorbance in the mid-IR region, this flow injection system was used for analysis of liquid samples by Bazin et al. [23] using the most prescribed drugs (n = 35) over 24 months. Although, the technique enabled 97% true recognition of molecules and 99.95% recognition of solvents, difficulties have been encountered in the discrimination of structurally related molecules: anthracyclines (doxorubicin, epirubicin and daunorubicin), oxazophosporines (cyclophosphamide and ifosfamide) as well as monoclonal antibodies (cetuximab, rituximab, trastuzumab and bevacizumab).

More recently, the focus shifted to Raman spectroscopy, considered more suited to liquid samples analysis [24]. A new generation of dedicated systems for AQC which combine UV/vis spectrometry with Raman spectroscopy has been commercialised (QCPrep+®, Icônes Service, France). The instrument is also a flow injection analyser, and has been progressively implemented in hospitals for AQC of small volume chemotherapeutic preparations. The method has been validated according to International Conference on Harmonisation (ICH) and resulted in a good quantification as well as identification of tested drugs [25]. Notably, a study conducted over 18 months at the University Hospital of Strasbourg (France) using a QCPrep+® analyser for AQC of 14 molecule-solvent combinations (ifosfamide, cyclophosphamide, doxorubicin, carboplatin, cisplatin, dacarbazine, docetaxel, etoposide, gemcitabine, oxaliplatin, paclitaxel, pemetrexed, vinorelbine) resulted in 99% identification of drugs and solvents while for quantitative analysis 1.52% of the preparations did not match the acceptance criteria, set to be ±15% [26].

Although Raman has great potential to ease the workload of AQC for preparation of chemotherapeutic solutions, one of the rising concerns is the safety of staff members manipulating molecules with carcinogenicity, mutagenicity and teratogenicity [27,28]. Therefore, non-invasive control directly into containers, i.e. without withdrawal and injection into a flow injection analyser, remains a current concern to be addressed.

The literature remains limited on the topic of AQC of chemotherapeutic solutions with Raman spectroscopy, a number of studies having been performed in glass vials [17,29–31]. Glass vials are useful models in research to demonstrate the potential of Raman spectroscopy, but have limited relevancy to support transfer of the technique into clinics, firstly because such glassware is never used to prepare individualised intravenous anticancer solutions, and secondly because transparent glass delivers a considerably different spectral signature to that of polymer or plastic based materials used in hospital infusion bags. Transfer of these technologies to the clinical environment is a slow process. Since the initial works published by Bourget et al. [4,21], who were first to highlight the potential of Raman spectroscopy for

analysis of anticancer solutions, there has been no significant development to further validate the technique for non-invasive analysis.

In 2014, Bourget et al. [32] documented a study about direct analysis of 5-fluorouracil prepared in elastomeric portable infusion pumps (1.5 - 50 $g \cdot L^{-1}$) using a RXN-1 Raman system (Kaiser Optical Systems, Ann Arbor, USA) in which the laser source (785nm) is connected via an optic fibre to the Raman illumination chamber (RIC). It is only recently, in 2019, that Lê *et al.* reported a follow up study for the AQC of gemcitabine directly in plastic bags using a handheld Raman instrument, in the range of concentrations from 1 – 20 $g \cdot L^{-1}$ [33]. These 2 publications clearly highlight the analytical potential of Raman analysis with (trans-) portable devices for transfer to the clinical environment for AQC of chemotherapeutic solutions. However, in terms of validation of the technique, a microscope based system enables acquisition from a specific point within the sample with the best definition of the sampled volume (i.e. voxel), and Confocal Raman Microspectroscopy (CRM) achieves the best precision in depth sampling compared non-confocal instruments. Therefore, CRM is chosen as the most suited approach to demonstrate the feasibility to perform *in situ* analysis as the foundation to then evaluate portable and handheld systems with reduced confocality.

The present study reports the investigation of CRM performed directly in infusion bags for AQC (discriminant and quantitative analysis) of three anticancer drugs (methotrexate, 5-fluorouracil and gemcitabine). Notably the prospects to develop a sensitive, reproducible and automated analytical method will be discussed.

2. Materials and Methods

2.1 Anticancer drugs

5% glucose infusion bags (Baxter, VIAFLO containers 50 mL, USA) and the 3 chemotherapeutic drugs used in this study have been provided through a collaboration with the UBCO unit (Unité de Biopharmacie Clinique Oncologique, Tours, France) that deals with the preparation of individualised chemotherapeutic doses at the University Hospital of Tours (CHU Tours, France).

Methotrexate (Mylan®, 100 $g \cdot L^{-1}$) is an antimetabolite that inhibits folic acid synthesis, hence inhibiting DNA synthesis and cell division [34–36]. It is used for the treatment of leukaemias, lymphomas, solid tumours, choriocarcinomas and rheumatoid arthritis [36,37].

5-fluorouracil (Accord®, 50 $g \cdot L^{-1}$) is a pyrimidine analogue that leads to DNA and RNA chain termination, and is used for treatment of gastrointestinal cancer, head, neck, pancreatic, colorectal and breast cancers [4,38,39]. Structurally, 5-fluorouracil is similar to uracil but one hydrogen atom is replaced by fluorine atom at carbon number 5 [40].

Gemcitabine (Sandoz®, 40 $g \cdot L^{-1}$) is a pyrimidine analogue used mainly for treatment of pancreatic adenocarcinomas as well as head, neck, breast ovarian and bladder cancers [41–44].

2.2 Raman spectroscopy analysis

a) Sample preparation for Raman in situ analysis

Based on track records of recently prepared solutions at UBCO, therapeutic ranges have been prepared for each drug. Sets of 6 concentrations (C1 to C6) have been prepared in 5% glucose directly into infusion bags using serial dilution. These were prepared within the clinical range of concentrations (Table 1). The procedure used was as follows: Firstly, an infusion bag containing 5% glucose was emptied using a syringe. Secondly, 5 mL of the highest concentration was prepared in a vial using micropipettes. Thirdly, 5 mL of the highest concentration were injected inside the empty infusion bag with a syringe (Concentration C1). Then for subsequent concentrations an appropriate volume of 5% glucose was added to the infusion bag to obtain the next targeted concentration within the range indicated in table 1 (Concentration C2). The last step is repeated 4 additional times to further dilute the solution inside the infusion bag and sequentially prepare concentrations C3, C4, C5 and C6. For the purpose of the study, each drug was prepared in 3 independent sets of 6 concentrations identified as SET_01, SET_02 (training) and SET_03 (testing). Each set of each drug was prepared in different infusion bags following the procedure described above. Throughout the study, samples are identified based on the drug contained in infusion bags as MTX (methotrexate), 5-FU (5-fluorouracil) and GEM (gemcitabine).

Table 1: Concentration range analysed

Drug	**Concentration range analysed (n = 6)**
MTX	3 $g \cdot L^{-1}$ – 21 $g \cdot L^{-1}$
5-FU	1 $g \cdot L^{-1}$ – 45 $g \cdot L^{-1}$
GEM	4 $g \cdot L^{-1}$ – 11 $g \cdot L^{-1}$

b) Data acquisition

Raman spectra were recorded using an Alpha300R Raman micro-spectrometer (WITec, Germany) equipped with a 532 nm diode laser set up to deliver 20 mW at the sample. The grating with 300 lines/mm was selected, delivering a spectral resolution of ~4 cm^{-1}. Spectra were collected over the range 300-1800 cm^{-1} thanks to a back illuminated deep depletion charged coupled device (CCD) detector. Every day, a calibration of the instrument for each laser line has been performed using the silica peak at 521 cm^{-1} prior to data collection.

1) Macro set up: A macro sampling cuvette holder (Horiba Jobin-Yvon, France) attached to the turret of the microscope has been used for recording using 500 µL of commercial stock solutions in quartz cuvette. Acquisition time was set to 2 accumulations of 30 seconds. *2) Microscope set up (confocal measurements):* Spectra have been collected using a x10 objective (Zeiss EC Epiplan-Neofluar Dic, NA=0.25 and 9.3 mm working distance). Additionally, the backscattered light is collected through a 10 µm diameter optical fibre, ensuring the high confocality of the measurements performed. Spectra resulted from 2 accumulations of 60 seconds and were collected. For each bag (SET_01, SET_02 and SET_03) and each concentration (n = 6), recording was made from 10 different positions on the bag, for total of 180 acquisition for each drug. For each position, the laser was focussed at the outer surface of the infusion bags and the position was set as 0 µm. Then, a Z scan was performed to automatically record spectra at 4 different depths, -300 µm, -500 µm, -700 µm and -900 µm.

c) Data handling

Raman data sets have been pre-processed and analysed using MATLAB® (Mathworks, USA). Data have been subjected to Extended Multiplicative Signal Correction (EMSC-toolbox) [45–47] followed the rubber band baseline correction [9].

Discriminant analysis: Partial Least Squares Discriminant Analysis (PLSDA) is a well-established supervised discriminant method. Presently, PLS2-DA was employed to perform the multiclass classification from the dataset. For each drug, 3 independent sets of data have been collected, SET_01, SET_02 and SET_03. SET_01 and SET_02 were used as training sets (n = 12), i.e. used for the construction of the model, while SET_03 was used solely as the test set (blind samples, n = 6). The training set is further divided into the calibration and validation sets. Therefore, calibration, validation and test sets are kept independent. The optimal number of latent variables (LVs) was selected with the validation set, while the outcome of the PLSDA represents the classification of samples from the test set. Ultimately, the results were presented in the form of confusion matrices, allowing calculation of the specificity and sensitivity of the discrimination achieved for the test set. For the purpose of this study each concentration has

been assigned to a different class to discriminate. The PLS-DA was therefore performed with 18 groups corresponding to the 3 drugs and the 6 concentrations prepared

Quantitative analysis: Partial Least Squares Regression (PLSR) has been applied in the fingerprint region (300 – 1800 cm^{-1}) to extract the relevant quantitative information concerning intensity to concentration relationship. Similar to PLSDA, for each drug, SET_01 (n = 6) and SET_02 (n = 6) were used as training sets while SET_03 was used as the test set (n = 6). The 12 samples of the combined training set were further separated in the calibration and validation sets. For the purpose of quantitative analysis, 2/3 of samples were randomly selected as the calibration set and the remaining 1/3 were used as validation set. A 100-fold iteration was implemented to evaluate the robustness of the analysis with multiple random combinations of calibration/validation sets. Notably, in all cases, the models were tested with SET_03, used as unknown samples to be determined. The output of this model gives information to evaluate the PLSR using the linearity of the regression between the measured and predicted concentrations (R^2), Root Mean Square Error of Cross Validation (RMSECV) calculated from the training datasets (SET_01 and SET_02), Root Mean Square Error of Prediction (RMSEP) calculated from the test set (i.e. Set 03) and the regression vector, which represents the variables (wavenumbers) used to create the regression model. In this study, the measured concentrations used as reference values for the construction of the PLSR models are determined using UV-Vis spectrophotometry (see section 2.2). Additionally, the lower Limit Of Detection (lower LOD) has been estimated based on the methodology of Allegrini et al. which established a mathematical model using the outcome of PLSR analysis [48].

2.3 UV/vis spectrometric analysis

a) Data acquisition

Absorbance was measured with a Genesys 10S UV–vis spectrophotometer (Thermo Scientific, France). Readings were taken at the wavelengths of maximum absorbance; 303 nm (MTX), 266 nm (5-FU) and 269 nm (GEM).

b) *Sample preparation for calibration curves*

In order to preserve the integrity of the infusion bags, the solutions were injected through the septum with a needle syringe. Because the volumes added cannot be known precisely, it was necessary to accurately determine the concentration of each solution prepared.

True concentrations were used as reference values for the PLSR analysis applied to Raman spectra (see section 2.4 Data handling). For this purpose, it has been necessary to first construct calibration curves. 5 standard solutions, each prepared in triplicate, were analysed for each drug (table 2). For each concentration the mean absorbance was calculated from triplicates and used for the construction of the calibration curve.

Table 2. Standard solutions prepared for the UV-Vis calibration curve

	GEM ($g.L^{-1}$)	5FU ($g.L^{-1}$)	MTX ($g.L^{-1}$)
Standard 1	0.055	0.06	0.0375
Standard 2	0.05	0.05	0.025
Standard 3	0.025	0.025	0.0125
Standard 4	0.0125	0.0125	0.00625
Standard 5	0.00625	0.00625	0.003125

Once the calibration curves are obtained, the concentration of samples prepared in infusion bags can be determined. For this purpose, after each injection of solutions in the infusion bags, the sample was homogenised by manual agitation and a small volume was withdrawn and analysed by UV-Vis spectrophotometry. Ultimately, reference concentrations for C1, C2, C3, C4, C5 and C6 were obtained for sets SET_01, SET_02 and SET_03 prepared for each drug.

3. Results

3.1 Spectral characterisation of infusion bags

Spectra from chemotherapeutics solutions in infusion bags have been collected using a confocal Raman micro-spectrometer using a x10 objective. The confocality of the Raman microscope enables to collect at defined focal depth, presently -300 µm, -500 µm, -700 µm and -900 µm. The depth of focus for the x10 objective lens is estimated to be ~140 µm using Berek Formula, taking into account the wavelength of the laser (532 nm) and the numerical aperture (NA = 0.25). Therefore, the aim is to find a position with the laser focus sufficiently inside the infusion bag where the spectral contribution from the materials of the bag is negligible compared to the signal originating from the solution. According to manufacturer specifications,

infusion bags used in this study are composed of polyolefin/polyamide co-extruded plastic; therefore a strong contribution can be expected in the Raman spectra collected. The thickness of the plastic wall of infusion bags observed by bright field microscopy is roughly 200 µm. This is confirmed with Figure 1a, which presents a typical mean Raman spectrum collected at depth -300µm. The spectrum exhibits strong contributions at 400 cm^{-1} (CH_2 wagging), 811 cm^{-1} (C-CH_3 stretching), 846 cm^{-1} (C-C backbone stretching), 1065 cm^{-1} (C-C backbone stretching), 1132 cm^{-1} (symmetric C-C stretching), 1174 cm^{-1} (C-H bending), 1298 cm^{-1} (CH_2 twisting), 1372 cm^{-1} (CH_3 symmetric bending), 1420 cm^{-1} (CH_2 bending), 1444 cm^{-1} (CH_2 bending), 1465 cm^{-1} (CH_2 asymmetric bending) and 1640 cm^{-1} (C=O stretching of the amide I from polyamide) all assigned to infusion bags materials [49–51]. However, Figure 1b, 1c and 1d highlights these features decrease significantly when recording is performed from respectively -500 µm, -700 µm, -900 µm. Clearly, it is possible to reduce the residual contribution from the infusion bag to reveal the features of the contents, in this case the OH bending of water, at 1640 cm^{-1}. Therefore, for subsequent analysis of chemotherapeutic solutions the depth – 900 µm has been preferred. Presently, no improvement was observed for higher depth of analysis with the instrumental set up used. Moreover, to avoid possible attenuation of the Raman signal for deeper focus of the laser inside the perfusion bags the Z position was kept as close as possible to the interface plastic-solution (i.e. -900 µm).

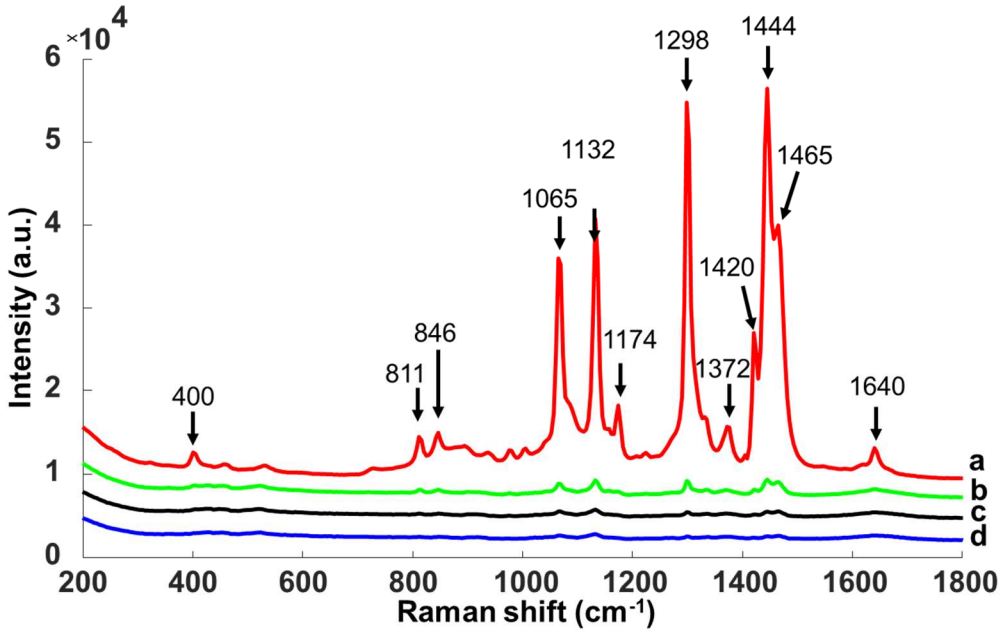

Figure 1: Mean Raman spectra of 5% glucose recorded through infusion bag at a) –300 µm (red), b) –500 µm (green), c) –700 µm (black) and d) –900 µm (blue) depth by 532 nm. Spectra are offset for clarity.

3.2 Spectral characterisation of anticancer drugs analysed

Figure 2 presents the mean Raman spectra obtained from commercial solutions of the 3 chemotherapeutic drugs analysed using the macro set up in quartz cuvettes (See 2. Materials and Methods). Figure 2a shows the mean spectrum of MTX, with characteristic bands at 679 cm^{-1} (aromatic C-C-C in plane bending), 715 cm^{-1} (C-C in plane bending), 772 cm^{-1} (C-C-N out of plane bending), 1215 cm^{-1} (C-NH_2 vibration), 1294 cm^{-1} (-CH_3 asymmetric deformation), 1359 cm^{-1} (CH_2 scissoring), 1384 cm^{-1} (-CH_3 symmetric deformation), 1457 cm^{-1} (C-N stretching), 1561 cm^{-1} (aromatic C-C stretching) and 1608 cm^{-1} (C-N stretching) [52–54]. Figure 2b shows the mean spectrum of 5-FU with features found at 364 cm^{-1} (out of plane ring bending), 487 cm^{-1} (in plane ring bending), 573 cm^{-1} (out of plane ring and C=O bending), 648 cm^{-1} (in plane ring bending), 772 cm^{-1} (pyrimidine ring breathing), 820 cm^{-1} (trigonal ring and C-F bending), 1014 cm^{-1} (C-H and N-H wagging), 1186 cm^{-1} (N-H in plane bending), 1232 cm^{-1} (ring and C-F bending), 1290 cm^{-1} (ring stretching), 1355 cm^{-1} (C-H wagging), 1616 cm^{-1} (trigonal ring mode) and 1679 cm^{-1} (symmetric C=O stretching) [55]. Finally, Figure 2c presents the mean spectrum of GEM with bands at 789 cm^{-1} (pyrimidine ring breathing), 824 cm^{-1} (C-F bending), 1261 cm^{-1} (ring stretching), 1457 cm^{-1} (CH_2 and CH_3 scissoring), 1545 cm^{-1} (C=C stretching) and 1659 cm^{-1} (hydrogen bonded C=O stretching) [17].
Unambiguously the 3 drugs display different Raman signatures with specific features enabling rapid identification.

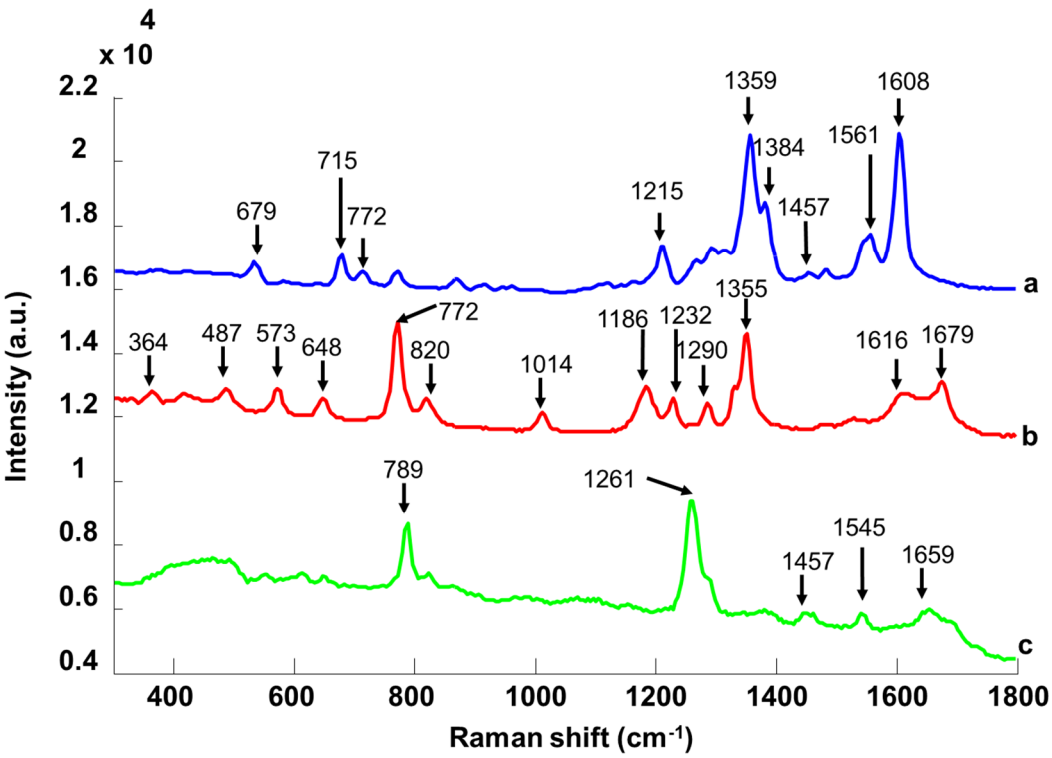

Figure 2: Mean Raman spectra recorded from concentrated stock solutions of a) MTX 100 g·L^{-1}, b) 5-FU 50 g·L^{-1} and c) GEM 40 g·L^{-1} by 532 nm. Spectra are offset for clarity.

3.3 Discriminant analysis

PLSDA has been applied to discriminate the spectra collected from solutions in infusion bags in the range of concentrations prepared for this study (see Table 1). Data were subjected to pre-processing prior to discriminant analysis. Presently, for each drug 3 sets of data have been collected, SET_01; SET_02 and SET_03. Firstly, the discriminative model was constructed using the training set composed of SET_01 and SET_02. Notably, separating the data into a calibration and validation set enables determination of the optimal number of latent variables, for instance n=3. Secondly, samples from SET_03 were analysed as an independent set of unknown samples (test set) to estimate the rate of classification for each drug.

Specificity and sensitivity of 100% were achieved for the test set (Table 3). The pure spectra collected from the 3 commercial drug solutions display distinct characteristic spectral signatures, (Figure 2), and therefore such an outcome can be expected.

Table 3: Specificity and sensitivity (%) obtained from PLSDA applied to the independent test SET_03 using 3 latent variables.

Drug	Specificity	Sensitivity
MTX	100	100
5-FU	100	100
GEM	100	100

Figure 3 presents the regression vectors obtained from PLSDA. The regression vector in Figure 3a presents negative features at 532 cm^{-1}, 680 cm^{-1}, 716 cm^{-1}, 772 cm^{-1}, 1216 cm^{-1}, 1360 cm^{-1}, 1384 cm^{-1}, 1560 cm^{-1} and 1608 cm^{-1} which are identical to MTX spectrum collected from stock solution (Figure 2a). The regression vector in Figure 3b presents negative features at 364 cm^{-1}, 492 cm^{-1}, 572 cm^{-1}, 652 cm^{-1}, 772 cm^{-1}, 824 cm^{-1}, 1016 cm^{-1}, 1188 cm^{-1}, 1232 cm^{-1}, 1292 cm^{-1}, 1684 cm^{-1} which are identical to 5-FU (Figure 2b). The regression vector in Figure 3c isn't directly comparable to spectrum of GEM (Figure 2c) however the 2 strong positive peaks at 789 cm^{-1} and 1261 cm^{-1} in addition to the weaker bands at 1545 cm^{-1} can be specifically assigned to the drug.

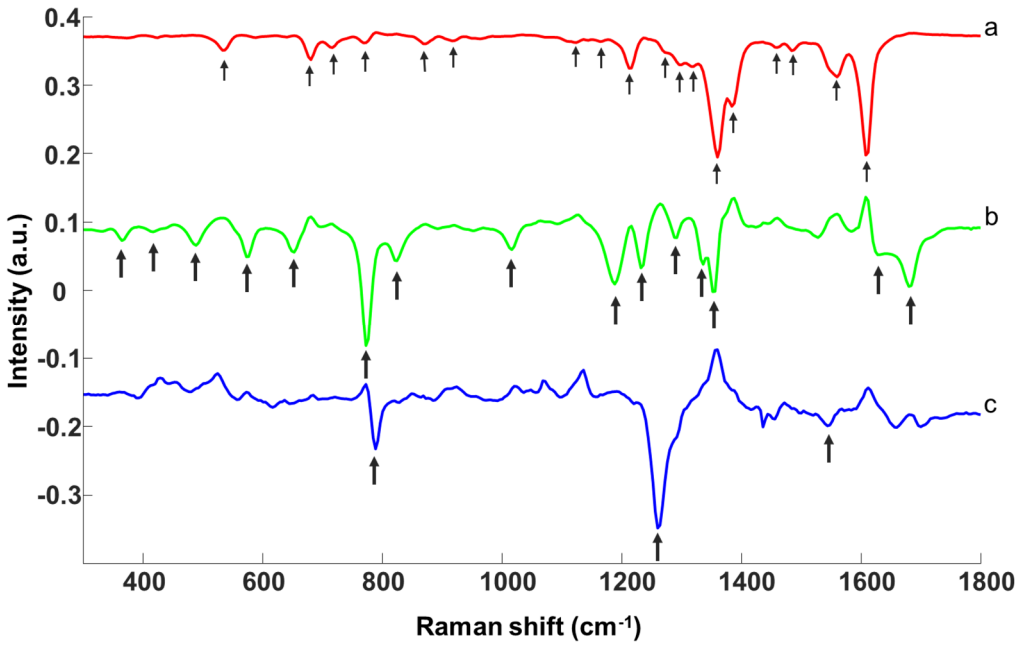

Figure 3: First (a), second (b) and third (c) regression vectors of PLSDA

3.3 Direct quantitative analysis in infusion bags

Figure 4 presents the mean Raman spectra collected for the 6 concentrations for MTX solutions inside infusion bags at the depth -900 µm. It is observed that spectral features of the drug proportionally decrease with the concentration of solutions. The data used for illustration in Figure 4 are from the first infusion bag analysed for MTX (i.e. Set_01), while the concentrations indicated, 20.1 $g \cdot L^{-1}$, 14.3 $g.L^{-1}$, 9.5 $g.L^{-1}$, 4.98 $g.L^{-1}$, 3.8 $g \cdot L^{-1}$ and 2.9 $g \cdot L^{-1}$, correspond to the quantification performed using UV-Vis absorbance (see 2. Materials and Methods). Mean spectra for GEM and 5-FU in 5% glucose in infusion are provided in supplementary material (Figure S1 and Figure S2).

The main challenge of the study was the preparation of samples directly into infusion bags at known concentration to enable the construction of PLSR models. While the aim is to demonstrate the feasibility to perform Raman analysis *in situ,* for the purpose of the study, withdrawal of a few microliters of the samples was necessary to perform UV-Vis spectrometry to determine accurately their concentration. This is achieved by the construction of 5 points calibration curves for each drug (see section 2.3). The concentrations of the solutions were determined to be 0.66±0.63% for MTX, 0.76±0.48% for 5FU and 1.98±2.29% for GEM using a calibrated UV-vis spectrophotometry procedure (see Supplementary materials, Figure S1, Figure S2 and Figure S3). The concentrations were used as reference concentrations (true concentrations) for PLSR analysis. These values can be used as reference concentrations (true concentrations) for PLSR analysis.

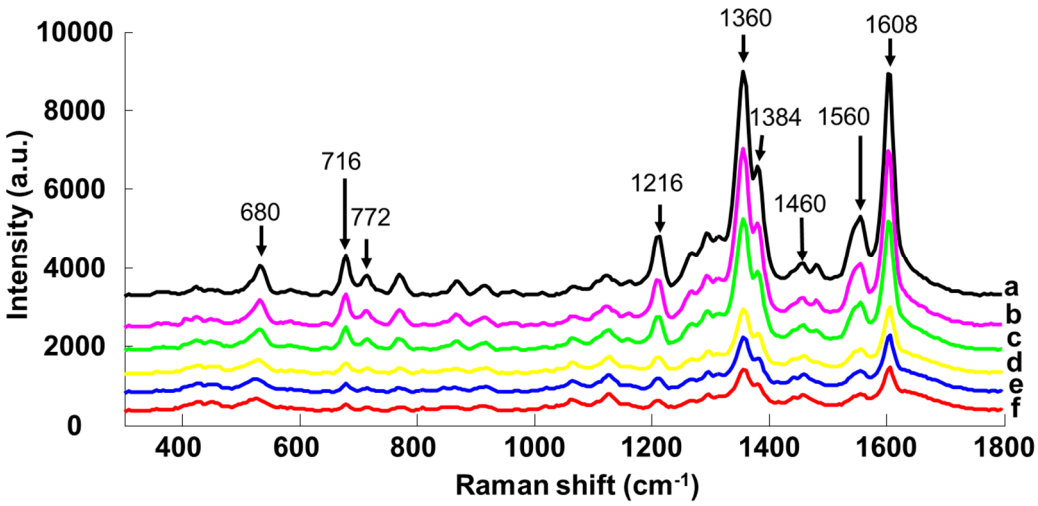

Figure 4: Mean Raman spectra of MTX in 5% glucose bag at –900 µm for respective concentrations of a) 20.1 $g.L^{-1}$, b) 14.3 $g.L^{-1}$, c) 9.5 $g.L^{-1}$, d) 4.98 $g.L^{-1}$, e) 3.8 $g.L^{-1}$ and f) 2.9 $g.L^{-1}$. Spectra are offset for clarity.

Figure 5 presents the results from PLSR of MTX performed using a calibration, validation and test set. The RMSECV calculated from the model constructed using the training set (Figure 5A) displays a slight decrease as a function of number of latent variables (LVs). It is observed that, above 3 LVs, no improvement of the accuracy can be reached. Figure 5B presents the correlation between predicted concentration and prepared concentration (measured with UV) obtained with the test set (SET_03). With a R^2 equal to 0.9951 and a RMSEP of 0.5280 g.L^{-1} it confirms the quality of the regression model. Table 4 summarises the PLSR results obtained with the test sets for the 3 drugs with RMSEP for 5-FU and GEM higher compared to MTX, respectively 1.5609 g.L^{-1} and 0.7772 g.L^{-1}. However, the higher values of RMSEP can reflect the differences in the range of concentration analysed (Table 1). The results can also be represented as the RMSEP expressed as percentage of the median concentration of the range tested. In this way, values of 5.8%, 8.2% and 10.2% for MTX, 5-FU and GEM are determined, respectively. It confirms the best accuracy is obtained for MTX followed by 5-FU and GEM. Additionally, the lower limit of detection (LOD) calculated from the PLSR analysis indicates that Raman directly in infusion bags enables determination of concentrations as low as 0.6469 g.L^{-1}, 0.6962 g.L^{-1} and 0.2895 g.L^{-1}, respectively for 5-FU, GEM and MTX. All 3 LOD are substantially lower than the lowest clinical concentration used in this study for these drugs (See table 1). While for 5-FU the LOD remains close to the lowest dose administered to patients for MTX it is nevertheless 10 times lower.

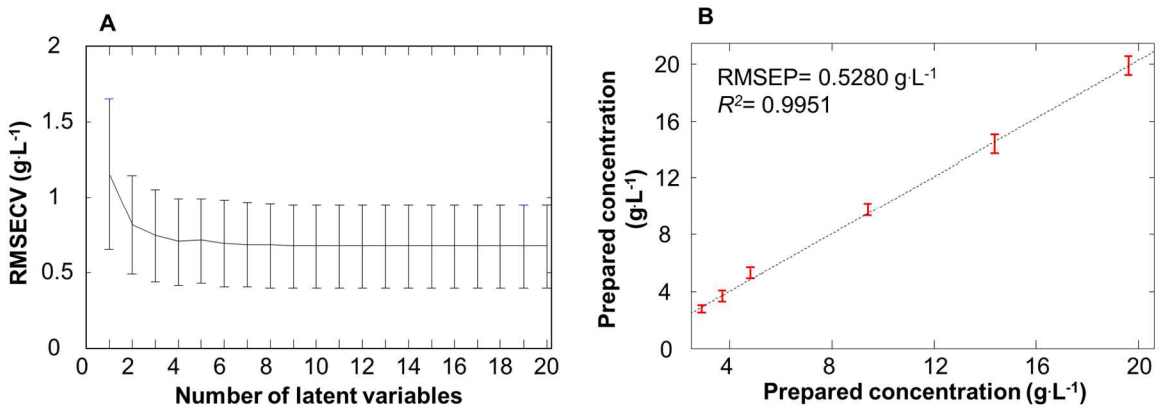

Figure 5: PLSR analysis performed on Raman data of MTX in 5% glucose bag recorded by 532 nm laser at -900 µm*: A) RMSECV (Training sets) and B) Regression plot with 4 LVs (test set).*

Table 4: Summary of PLSR results obtained with the test sets at depth -900 µm

Drug	LVs	R^2	RMSEP ($g \cdot L^{-1}$)	% RMSEP
MTX	3	0.9951	0.5280	5.8
5-FU	2	0.9947	1.5609	8.2
GEM	4	0.9181	0.7772	10.2

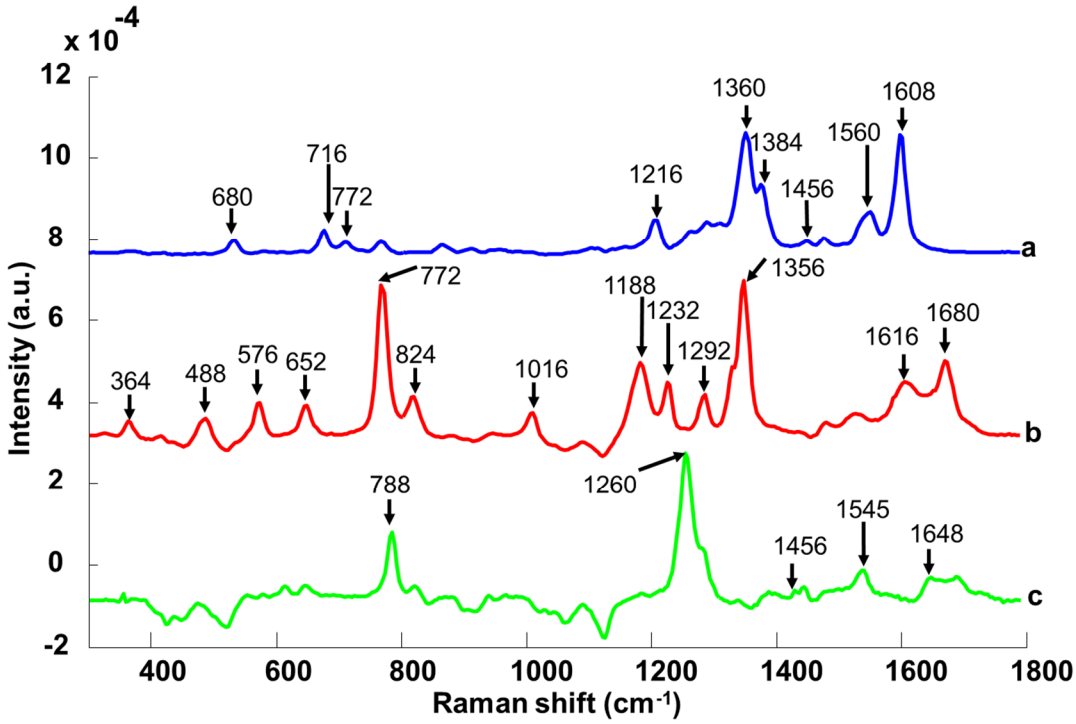

Figure 6: First regression vectors of PLSR for a) MTX, b) 5-FU and c) GEM. Spectra are offset for clarity.

Regression vectors (Figure 6) highlight the spectral features used in the quantitative models constructed with PLSR. For MTX (Figure 6a), bands at 680 cm^{-1}, 716 cm^{-1}, 772 cm^{-1}, 1216 cm^{-1}, 1360 cm^{-1}, 1384 cm^{-1}, 1456 cm^{-1}, 1560 cm^{-1} and 1608 cm^{-1} are characteristic of MTX and resemble those observed in Figure 2a. This illustrates the specificity of quantification which is performed on MTX bands. Similarly, Figure 6b presents characteristic bands of 5-FU at 364 cm^{-1}, 488 cm^{-1}, 576 cm^{-1}, 652 cm^{-1}, 772 cm^{-1}, 824 cm^{-1}, 1016 cm^{-1}, 1188 cm^{-1}, 1232 cm^{-1}, 1292 cm^{-1}, 1356 cm^{-1}, 1616 cm^{-1} and 1680 cm^{-1} which coincide with that obtained in Figure 2b.

Finally Figure 5c, presents peaks of GEM at 788 cm^{-1}, 1260 cm^{-1}, 1456 cm^{-1}, 1548 cm^{-1} and 1656 cm^{-1} which are the characteristic features observed in Figure 2c.

Unambiguously, Raman analysis in infusion bags coupled to PLSR analysis enables correlation of spectral variations with concentrations of chemotherapeutic solutions. In addition to quality of the fitting model constructed by PLSR, the estimated concentrations can be extracted to evaluate accuracy of prediction. Table 5 summarises the errors (expressed as percentage) in the estimated concentrations with Raman spectroscopy compared to the reference concentrations obtained with UV-Vis spectroscopy. C1 refers to the lowest concentration of the target range while C6 is the highest. Notably, there is no clear legislation regarding the acceptance criteria for individualised chemotherapeutic solutions. As an example, the centralised unit at the University Hospital of Tours has a 10% tolerance in the quantification of drugs in final solutions. However, in the literature, some studies report acceptance criteria up to 15% [26]. In the current study, it is observed that MTX and GEM display errors in predicted concentrations significantly below the 10% threshold, the highest error found to be 6.5%. For 5-FU, errors between 5.9% and 18.5% are found for the 3 lowest concentrations, while for the 3 highest, the % error greatly decreases to, respectively, 1.2%, 2% and 2.9% for C4, C5 and C6.

Table 5: Summary of %error in predicted concentrations (Raman spectroscopy) compared to reference concentrations (UV-Vis absorbance) for the test set.

Concentration	MTX	5-FU	GEM
C1	6.5%	18.5%	0.77%
C2	3.7%	11.4%	1.2%
C3	5.6%	5.9%	1.4%
C4	2.7%	1.2%	1.6%
C5	0.49%	2%	2.2%
C6	0.89%	2.9%	3.7%

4. General Discussion

Confocality of Raman microspectroscopic analysis, when performed with suitable instruments, is a well-established a valuable strength of the technique used in numerous applications in the biomedical and pharmaceutical fields [7,56,57]. Over the last decade, the development of compact benchtop Raman spectrometer equipped with remote confocal probes connected with

optical fibres have greatly contributed to increasing the attractiveness of Raman spectroscopy for direct analysis of solutions or powders contained within glassware or other containers [58,59]. It is particularly suited for quality control of raw materials or solvents in the pharmaceutical industry [13]. Nowadays, miniaturisation and compaction of analytical devices is a strong marketing trend, the range of portable systems now including handheld Raman devices [31]. However, to date, no benchmarking has been set to clearly demonstrate the instrumental set up delivering the optimal analytical output for quantification and discrimination of chemotherapeutic solutions, also considering other parameters such as cost of purchase, maintenance or ergonomic design.

Clearly there is a lack of consensus to date about the appropriate application of *in situ* Raman spectroscopy to ACQ in infusion bags. The instrumental and experimental set ups, notably wavelength of laser, spectral resolution and drug analysed, make a direct comparison of previously published data to the present study difficult. As a consequence, only three referenced studies in the literature are used to provide an overview of the state of the art of applications of CRM to ACQ.

In terms of analytical performances, the RMSEP of 0.7772 $g \cdot L^{-1}$ found presently for GEM with CRM is comparable to the output of the previous study published by Le et al. [17] who reported an RMSEP of 0.79 $g \cdot L^{1}$ for analysis in glass vials. The slight difference can be explained by differences in the range of concentrations analysed, respectively 4 -11 $g \cdot L^{-1}$ and 1 -20 $g \cdot L^{-1}$. The recent study from Lê et al. [33] using handheld Raman reported a RMSEP of 0.76 $g \cdot L^{-1}$ for analysis directly in infusion bags. However, it is important to mention that the commercial gemcitabine solution used was from Mylan®, which is prepared in ethanol, while the brand used in the present study is Sandoz®, without ethanol. Ethanol is a relatively strong Raman scatterer, which contributes strongly to the data collected [33], therefore improving the PLSR fitting. The lack of consistency between experimental designs can give rise to diversity in the outcomes and, notably, the influence of the laser power and the wavelength used on the signal to noise ratio make direct comparison difficult. For 5-FU, the RMSEP of 1.5609 $g \cdot L^{-1}$ found with CRM appears superior to the value of 0.379 $g.L^{-1}$ reported by Bourget et al. in elastomeric infusion pumps [4] however lower than 3.05 $g.L^{-1}$ of the study of Le *at al.* in a glass vial [17]. Although the type of containers can be a crucial parameter influencing the quality of the fitting achieved, there is no evidence that differences are related to the instrumental set up, the collection efficiency (sample presentation), range of concentration selected or number of samples in the calibration / validation sets. Despite the differences in RMSEP, the errors in predicted concentrations measured here are below 11.4% for 5-FU except for the lowest

concentration which is 18.5%, and therefore significantly within the range of the 10-15% acceptance criteria commonly defined in studies. Therefore, the results presently collected with CRM are encouraging and highlight the reliability of analysis performed. However, the investigation remains preliminary and a more extended panel of molecules should be included to provide an in-depth investigation of direct, non-invasive, analysis in infusion bags.

In terms of applications potential, the repeatability and reproducibility of the measurement process could be further refined by automated sample positioning and light collection. For instance, commercialised Raman microscopes commonly include functionalities for autofocus that can be used to repeatedly set the 0 position at the surface of the bags. Therefore, a software protocol to automatically increment a pre-defined movement to focus the laser inside the infusion bag is readily achievable. Moreover, CRM can be purchased with an inverted set up (objective lens pointing toward the ceiling) that can be used for liquid samples analysis [61,62]. It implies pharmacists or technicians would have to simply place the bag on top of the motorised stage then the process of data collection would be automated thus significantly faster and reproducible. A dedicated inverted Raman microscope with a simplified configuration would be competitive cost wise with other benchtop systems and handhelds devices that remain relatively expensive technologies.

Ultimately, a number of parameters should be considered and compared to fully address the suitability of each instrument for AQC. The present preliminary study clearly demonstrates the feasibility to quantify and discriminate 3 common drugs, gemcitabine, 5-fluorouracile and methotrexate, directly inside infusion bags. Developing CRM for AQC of chemotherapeutic solution should therefore be considered as one of suitable options.

5. Conclusion

Raman spectroscopy applied to AQC of chemotherapeutic drugs in infusion bags delivers mean relative error in predicted concentrations of 3.31%, 6.98% and 1.81%, respectively for MTX, 5FU and GEM. Considering the acceptance criteria of 10%, the technique is an accurate tool for *in situ*, rapid and cost-effective, label free analysis of individualised anticancer solutions. Performing analysis without withdrawal of solutions it a major step forward to ensure the safety of staff members of centralised preparation units. Moreover, the technique conforms to current requirements for molecular specificity enabling 100% discrimination of MTX, 5-FU and GEM solutions. While the literature remains scarce on the topic of non-invasive analysis, there is no doubt that Raman spectroscopy has the potential to be used as routine protocol for AQC, at

least for a selected number of molecules with strong spectral response. Moreover, Confocal Raman Microscopy offers attractive analytical performances in terms of reproducibility of analysis performed through in infusion bag materials, thanks to the high confocality of microscope. Such set up could be rapidly automated and readily transferable in centralised units to provide a next generation of AQC tools for routine analysis.

Acknowledgement

Campus France and French embassy in Sudan for financial support for PhD in cotutelle between University of Gezira and University of Tours.

Bibliography

[1] L. Vinet, A. Zhedanov, A "missing" family of classical orthogonal polynomials, J. Phys. A Math. Theor. 44 (2011) 1039–1042. https://doi.org/10.1088/1751-8113/44/8/085201.

[2] M. Savelli, M. Roche, C. Curti, C. Bornet, P. Rathelot, M. Montana, P. Vanelle, Methods to control anticancer chemotherapy preparations ranked by risk analysis, Pharmazie. 73 (2018) 251–259. https://doi.org/10.1691/ph.2018.7205.

[3] A. Delmas, J.B. Gordien, J.M. Bernadou, M. Roudaut, A. Gresser, L. Malki, M.C. Saux, D. Breilh, Quantitative and qualitative control of cytotoxic preparations by HPLC-UV in a centralized parenteral preparations unit, J. Pharm. Biomed. Anal. 49 (2009) 1213–1220. https://doi.org/10.1016/j.jpba.2009.03.007.

[4] P. Bourget, A. Amin, F. Vidal, C. Merlette, F. Lagarce, Comparison of Raman spectroscopy vs. high performance liquid chromatography for quality control of complex therapeutic objects: Model of elastomeric portable pumps filled with a fluorouracil solution, J. Pharm. Biomed. Anal. 91 (2014) 176–184. https://doi.org/10.1016/j.jpba.2013.12.030.

[5] I. Badea, L. Lazăr, D. Moja, D. Nicolescu, A. Tudose, A HPLC method for the simultaneous determination of seven anthracyclines, J. Pharm. Biomed. Anal. 39 (2005) 305–309. https://doi.org/10.1016/j.jpba.2005.03.039.

[6] E. Gravel, P. Bourget, L. Mercier, A. Paci, Fluorescence detection combined with either HPLC or HPTLC for pharmaceutical quality control in a hospital chemotherapy production unit: Application to camptothecin derivatives, J. Pharm. Biomed. Anal. 39 (2005) 581–586. https://doi.org/10.1016/j.jpba.2005.05.010.

[7] L.M. Moreira, L. Silveira, F. V. Santos, J.P. Lyon, R. Rocha, R.A. Zângaro, A.B. Villaverde, M.T.T. Pacheco, Raman spectroscopy: A powerful technique for biochemical analysis and diagnosis, Spectroscopy. 22 (2008) 1–19. https://doi.org/10.3233/SPE-2008-0326.

[8] L. Miloudi, F. Bonnier, A. Tfayli, F. Yvergnaux, H.J. Byrne, I. Chourpa, E. Munnier, Confocal Raman spectroscopic imaging for in vitro monitoring of active ingredient penetration and distribution in reconstructed human epidermis model, J. Biophotonics. 11 (2018) 1–17. https://doi.org/10.1002/jbio.201700221.

[9] F. Bonnier, G. Brachet, R. Duong, T. Sojinrin, R. Respaud, N. Aubrey, M.J. Baker, H.J. Byrne, I. Chourpa, Screening the low molecular weight fraction of human serum using ATR-IR spectroscopy, J. Biophotonics. 9 (2016) 1085–1097. https://doi.org/10.1002/jbio.201600015.

[10] B. Van Eerdenbrugh, L.S. Taylor, Application of mid-IR spectroscopy for the characterization of pharmaceutical systems, Int. J. Pharm. 417 (2011) 3–16. https://doi.org/10.1016/j.ijpharm.2010.12.011.

[11] R. Gasper, J. Dewelle, R. Kiss, T. Mijatovic, E. Goormaghtigh, IR spectroscopy as a new tool for evidencing antitumor drug signatures, Biochim. Biophys. Acta - Biomembr. 1788 (2009) 1263–1270. https://doi.org/10.1016/j.bbamem.2009.02.016.

[12] K. Kong, C. Kendall, N. Stone, I. Notingher, Raman spectroscopy for medical diagnostics - From in-vitro biofluid assays to in-vivo cancer detection, Adv. Drug Deliv. Rev. 89 (2015) 121–134. https://doi.org/10.1016/j.addr.2015.03.009.

[13] R.S. Das, Y.K. Agrawal, Raman spectroscopy: Recent advancements, techniques and applications, Vib. Spectrosc. 57 (2011) 163–176. https://doi.org/10.1016/j.vibspec.2011.08.003.

[14] L.P. Choo-Smith, H.G.M. Edwards, H.P. Endtz, J.M. Kros, F. Heule, H. Barr, J.S. Robinson, H.A. Bruining, G.J. Puppels, Medical applications of Raman spectroscopy: From proof of principle to clinical implementation, Biopolym. - Biospectroscopy Sect. 67 (2002) 1–9. https://doi.org/10.1002/bip.10064.

[15] D.I. Ellis, D.P. Cowcher, L. Ashton, S. O'Hagan, R. Goodacre, Illuminating disease and enlightening biomedicine: Raman spectroscopy as a diagnostic tool, Analyst. 138 (2013) 3871–3884. https://doi.org/10.1039/c3an00698k.

[16] Z. Movasaghi, S. Rehman, I.U. Rehman, Raman spectroscopy of biological tissues, Appl. Spectrosc. Rev. 42 (2007) 493–541. https://doi.org/10.1080/05704920701551530.

[17] L.M.M. Lê, M. Berge, A. Tfayli, J. Zhou, P. Prognon, A. Baillet-Guffroy, E. Caudron, Rapid discrimination and quantification analysis of five antineoplastic drugs in aqueous solutions using Raman spectroscopy, Eur. J. Pharm. Sci. 111 (2018) 158–166. https://doi.org/10.1016/j.ejps.2017.09.046.

[18] V. Balan, C.T. Mihai, F.D. Cojocaru, C.M. Uritu, G. Dodi, D. Botezat, I. Gardikiotis, Vibrational spectroscopy fingerprinting in medicine: From molecular to clinical practice, Materials (Basel). 12 (2019) 1–40. https://doi.org/10.3390/ma12182884.

[19] F. Dziopa, G. Galy, S. Bauler, B. Vincent, S. Crochon, M.L. Tall, F. Pirot, C. Pivot, A quantitative and qualitative method to control chemotherapeutic preparations by Fourier transform infrared-ultraviolet spectrophotometry, J. Oncol. Pharm. Pract. 19 (2013) 121–129. https://doi.org/10.1177/1078155212457963.

[20] C. Bazin, V. Vieillard, A. Astier, M. Paul, Implementation of real-time identification analysis and quantification of chemotherapies preparations with a Multispec® analyser, Ann. Pharm. Fr. 72 (2014) 33–40. https://doi.org/10.1016/j.pharma.2013.09.006.

[21] P. Bourget, A. Amin, F. Vidal, C. Merlette, P. Troude, A. Baillet-Guffroy, The contribution of Raman spectroscopy to the analytical quality control of cytotoxic drugs in a hospital environment: Eliminating the exposure risks for staff members and their work environment, Int. J. Pharm. 470 (2014) 70–76. https://doi.org/10.1016/j.ijpharm.2014.04.064.

[22] P. Bourget, A. Amin, A. Moriceau, B. Cassard, F. Vidal, R. Clement, La Spectroscopie Raman (SR): Un nouvel outil adapté au contrôle de qualité analytique des préparations injectables en milieu de soins. Comparaison de la SR aux techniques CLHP et UV/visible-IRTF appliquée à la classe des anthracyclines en canct, Pathol. Biol. 60 (2012) 369–379. https://doi.org/10.1016/j.patbio.2011.10.010.

[23] C. Bazin, V. Vieillard, A. Astier, M. Paul, Implementation of real-time identification analysis and quantification of chemotherapies preparations with a Multispec® analyser, Ann. Pharm. Fr. 72 (2014) 33–40. https://doi.org/10.1016/j.pharma.2013.09.006.

[24] A.A. Makki, F. Bonnier, R. Respaud, F. Chtara, A. Tfayli, C. Tauber, D. Bertrand, H.J. Byrne, E. Mohammed, I. Chourpa, Qualitative and quantitative analysis of therapeutic solutions using Raman and infrared spectroscopy, Spectrochim. Acta - Part A Mol. Biomol. Spectrosc. 218 (2019) 97–108. https://doi.org/10.1016/j.saa.2019.03.056.

[25] T. Chouquet, G. Benoit, K. Morand, Implementation of Analytical Control of Low

Volume Pediatric Cytotoxic Drugs Preparations using a UV/Raman Spectrophotometer, Pharm. Technol. Hosp. Pharm. 1 (2016) 151–162. https://doi.org/10.1515/pthp-2016-0013.

[26] F. Nardella, M. Beck, P. Collart-Dutilleul, G. Becker, C. Boulanger, L. Perello, A. Gairard-Dory, B. Gourieux, G. Ubeaud-Séquier, A UV-Raman spectrometry method for quality control of anticancer preparations: Results after 18 months of implementation in hospital pharmacy, Int. J. Pharm. 499 (2016) 343–350. https://doi.org/10.1016/j.ijpharm.2016.01.002.

[27] C.B.P. da Silva, I.P. Julio, G.E. Donadel, I. Martins, UPLC-MS/MS method for simultaneous determination of cyclophosphamide, docetaxel, doxorubicin and 5-fluorouracil in surface samples, J. Pharmacol. Toxicol. Methods. 82 (2016) 68–73. https://doi.org/10.1016/j.vascn.2016.08.004.

[28] C. Rioufol, F. Ranchon, V. Schwiertz, N. Vantard, E. Joue, C. Gourc, N. Gauthier, M.G. Guedat, G. Salles, P.J. Souquet, B. Favier, L. Gilles, G. Freyer, B. You, V. Trillet-Lenoir, J. Guitton, Administration of anticancer drugs: Exposure in hospital nurses, Clin. Ther. 36 (2014) 401–407. https://doi.org/10.1016/j.clinthera.2014.01.016.

[29] A. Amin, P. Bourget, F. Vidal, F. Ader, Routine application of Raman spectroscopy in the quality control of hospital compounded ganciclovir, Int. J. Pharm. 474 (2014) 193–201. https://doi.org/10.1016/j.ijpharm.2014.08.028.

[30] L.M.M. Lê, A. Tfayli, J. Zhou, P. Prognon, A. Baillet-Guffroy, E. Caudron, Discrimination and quantification of two isomeric antineoplastic drugs by rapid and non-invasive analytical control using a handheld Raman spectrometer, Talanta. 161 (2016) 320–324. https://doi.org/10.1016/j.talanta.2016.07.025.

[31] L. Lê, M. Berge, A. Tfayli, P. Prognon, E. Caudron, Discriminative and Quantitative Analysis of Antineoplastic Taxane Drugs Using a Handheld Raman Spectrometer, Biomed Res. Int. 2018 (2018) 12–15. https://doi.org/10.1155/2018/8746729.

[32] P. Bourget, A. Amin, F. Vidal, C. Merlette, F. Lagarce, Comparison of Raman spectroscopy vs. high performance liquid chromatography for quality control of complex therapeutic objects: Model of elastomeric portable pumps filled with a fluorouracil solution, J. Pharm. Biomed. Anal. 91 (2014) 176–184. https://doi.org/10.1016/j.jpba.2013.12.030.

[33] L. Lê, M. Berge, A. Tfayli, A. Baillet Guffroy, P. Prognon, A. Dowek, E. Caudron, Quantification of gemcitabine intravenous drugs by direct measurement in chemotherapy plastic bags using a handheld Raman spectrometer, Talanta. 196 (2019)

376–380. https://doi.org/10.1016/j.talanta.2018.11.062.
[34] I. Rodin, A. Braun, A. Stavrianidi, O. Shpigun, A validated LC-MS/MS method for rapid determination of methotrexate in human saliva and its application to an excretion evaluation study, J. Chromatogr. B Anal. Technol. Biomed. Life Sci. 937 (2013) 1–6. https://doi.org/10.1016/j.jchromb.2013.07.026.
[35] E. Dickens, S. Ahmed, Principles of cancer treatment by chemotherapy, Surg. (United Kingdom). 36 (2018) 134–138. https://doi.org/10.1016/j.mpsur.2017.12.002.
[36] S. Nussbaumer, P. Bonnabry, J.L. Veuthey, S. Fleury-Souverain, Analysis of anticancer drugs: A review, Talanta. 85 (2011) 2265–2289. https://doi.org/10.1016/j.talanta.2011.08.034.
[37] D.M. Bach, J.A. Straseski, W. Clarke, Therapeutic drug monitoring in cancer chemotherapy, Bioanalysis. 2 (2010) 863–879. https://doi.org/10.4155/bio.10.48.
[38] A.A. Thoppil, S. Choudhary, N. Kishore, Competitive binding of anticancer drugs 5-fluorouracil and cyclophosphamide with serum albumin: Calorimetric insights, Biochim. Biophys. Acta - Gen. Subj. 1860 (2016) 917–929. https://doi.org/10.1016/j.bbagen.2016.01.026.
[39] E.J.B. Derissen, M.J.X. Hillebrand, H. Rosing, J.H.M. Schellens, J.H. Beijnen, Development of an LC-MS/MS assay for the quantitative determination of the intracellular 5-fluorouracil nucleotides responsible for the anticancer effect of 5-fluorouracil, J. Pharm. Biomed. Anal. 110 (2015) 58–66. https://doi.org/10.1016/j.jpba.2015.02.051.
[40] H.K. Risinggård, S. Cooil, F. Mazzola, D. Hu, M. Kjærvik, E.R. Østli, N. Patil, A. Preobrajenski, D. Andrew Evans, D.W. Breiby, T.T. Trinh, J.W. Wells, Degradation of the chemotherapy drug 5-fluorouracil on medical-grade silver surfaces, Appl. Surf. Sci. 435 (2018) 1213–1219. https://doi.org/10.1016/j.apsusc.2017.11.221.
[41] J. Ciccolini, C. Serdjebi, G.J. Peters, E. Giovannetti, Pharmacokinetics and pharmacogenetics of Gemcitabine as a mainstay in adult and pediatric oncology: an EORTC-PAMM perspective, Cancer Chemother. Pharmacol. 78 (2016) 1–12. https://doi.org/10.1007/s00280-016-3003-0.
[42] C.M. Li, L. Zhang, Y.H. Hou, N. Li, M.H. Che, Targeted delivery of gemcitabine to pancreatic adenocarcinoma using anti-EGFR antibody as a targeting agent, World Chinese J. Dig. 23 (2015) 1890–1896. https://doi.org/10.11569/wcjd.v23.i12.1890.
[43] O. Caffo, S. Fallani, E. Marangon, S. Nobili, M.I. Cassetta, V. Murgia, F. Sala, A. Novelli, E. Mini, M. Zucchetti, E. Galligioni, Pharmacokinetic study of gemcitabine,

given as prolonged infusion at fixed dose rate, In combination with cisplatin In patients with advanced non-small-cell lung cancer, Cancer Chemother. Pharmacol. 65 (2010) 1197–1202. https://doi.org/10.1007/s00280-010-1255-7.

[44] K.Y. Hsu, W.H. Hao, J.J. Wang, S.P. Hsueh, P.J. Hsu, L.C. Chang, C.S. Hsu, In vitro and in vivo studies of pharmacokinetics and antitumor efficacy of D07001-F4, an oral gemcitabine formulation, Cancer Chemother. Pharmacol. 71 (2013) 379–388. https://doi.org/10.1007/s00280-012-2017-5.

[45] L.E. Jamieson, H.J. Byrne, Vibrational spectroscopy as a tool for studying drug-cell interaction: Could high throughput vibrational spectroscopic screening improve drug development?, Vib. Spectrosc. 91 (2017) 16–30. https://doi.org/10.1016/j.vibspec.2016.09.003.

[46] P. dos Santos Panero, F. dos Santos Panero, J. dos Santos Panero, H.E. Bezerra da Silva, Application of Extended Multiplicative Signal Correction to Short-Wavelength near Infrared Spectra of Moisture in Marzipan, J. Data Anal. Inf. Process. 01 (2013) 30–34. https://doi.org/10.4236/jdaip.2013.13005.

[47] Q. Li, Q. Gao, G. Zhang, Improved extended multiplicative scatter correction algorithm applied in blood glucose noninvasive measurement with FT-IR spectroscopy, J. Spectrosc. (2013) 1–6. https://doi.org/10.1155/2013/916351.

[48] F. Allegrini, A.C. Olivieri, IUPAC-consistent approach to the limit of detection in partial least-squares calibration, Anal. Chem. 86 (2014) 7858–7866. https://doi.org/10.1021/ac501786u.

[49] E. Andreassen, Infrared and Raman spectroscopy of polypropylene, (1999) 320–328. https://doi.org/10.1007/978-94-011-4421-6_46.

[50] M. Zou, B. Barton, G. Geertz, R. Brüll, Accurate determination of the layer thickness of a multilayer polymer film by non-invasive multivariate confocal Raman microscopy, Analyst. 144 (2019) 5600–5607. https://doi.org/10.1039/c9an00664h.

[51] H. Sato, S. Sasao, K. Matsukawa, Y. Kita, T. Ikeda, H. Tashiro, Y. Ozaki, Raman mapping study of compatibilized and uncompatibilized polymer blends of Nylon 12 and polyethylene, Appl. Spectrosc. 56 (2002) 1038–1043. https://doi.org/10.1366/000370202321274845.

[52] S. Ayyappan, N. Sundaraganesan, V. Aroulmoji, E. Murano, S. Sebastian, Molecular structure, vibrational spectra and DFT molecular orbital calculations (TD-DFT and NMR) of the antiproliferative drug Methotrexate, Spectrochim. Acta - Part A Mol. Biomol. Spectrosc. 77 (2010) 264–275. https://doi.org/10.1016/j.saa.2010.05.021.

[53] I.J. Hidi, A. Mühlig, M. Jahn, F. Liebold, D. Cialla, K. Weber, J. Popp, LOC-SERS: Towards point-of-care diagnostic of methotrexate, Anal. Methods. 6 (2014) 3943–3947. https://doi.org/10.1039/c3ay42240b.

[54] D.R. Parachalil, D. Commerford, F. Bonnier, I. Chourpa, J. McIntyre, H.J. Byrne, Raman spectroscopy as a potential tool for label free therapeutic drug monitoring in human serum: The case of busulfan and methotrexate, Analyst. 144 (2019) 5207–5214. https://doi.org/10.1039/c9an00801b.

[55] S. Farquharson, A. Gift, C. Shende, F. Inscore, B. Ordway, C. Farquharson, J. Murren, Surface-enhanced Raman spectral measurements of 5-fluorouracil in saliva, Molecules. 13 (2008) 2608–2627. https://doi.org/10.3390/molecules13102608.

[56] H.J. Butler, L. Ashton, B. Bird, G. Cinque, K. Curtis, J. Dorney, K. Esmonde-White, N.J. Fullwood, B. Gardner, P.L. Martin-Hirsch, M.J. Walsh, M.R. McAinsh, N. Stone, F.L. Martin, Using Raman spectroscopy to characterize biological materials, Nat. Protoc. 11 (2016) 664–687. https://doi.org/10.1038/nprot.2016.036.

[57] K.A. Esmonde-White, M. Cuellar, C. Uerpmann, B. Lenain, I.R. Lewis, Raman spectroscopy as a process analytical technology for pharmaceutical manufacturing and bioprocessing, Anal. Bioanal. Chem. 409 (2017) 637–649. https://doi.org/10.1007/s00216-016-9824-1.

[58] A. Paudel, D. Raijada, J. Rantanen, Raman spectroscopy in pharmaceutical product design, Adv. Drug Deliv. Rev. 89 (2015) 3–20. https://doi.org/10.1016/j.addr.2015.04.003.

[59] B. Gotter, W. Faubel, R.H.H. Neubert, FTIR microscopy and confocal Raman microscopy for studying lateral drug diffusion from a semisolid formulation, Eur. J. Pharm. Biopharm. 74 (2010) 14–20. https://doi.org/10.1016/j.ejpb.2009.07.006.

[60] T. Chouquet, G. Benoit, K. Morand, Analytical Control of Pediatric Chemotherapy Preparations with a UV-Raman Automaton: Results After 18 Months of Implementation and Development of A Suitable Method for Low Volume Preparations, Pharm. Technol. Hosp. Pharm. 2 (2017) 117–129. https://doi.org/10.1515/pthp-2017-0021.

[61] D.R. Parachalil, C. Bruno, F. Bonnier, H. Blasco, I. Chourpa, J. McIntyre, H.J. Byrne, Raman spectroscopic screening of high and low molecular weight fractions of human serum, Analyst. 144 (2019) 4295–4311. https://doi.org/10.1039/c9an00599d.

[62] F. Bonnier, F. Petitjean, M.J. Baker, H.J. Byrne, Improved protocols for vibrational spectroscopic analysis of body fluids, J. Biophotonics. 7 (2014) 167–179.

https://doi.org/10.1002/jbio.201300130.

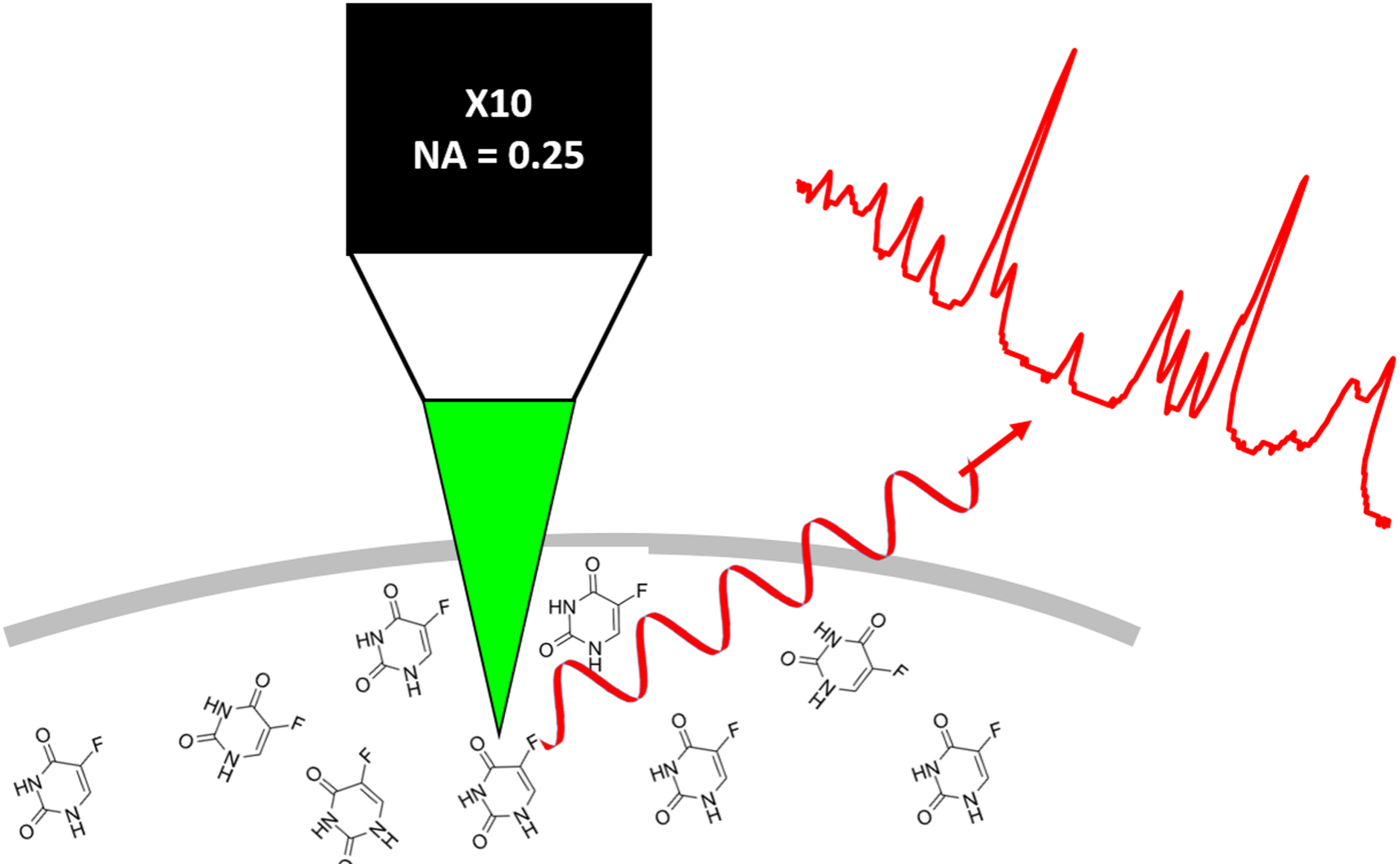
X10
NA = 0.25